Design and Synthesis of stable Porous Materials for Sensing Applications

Thesis report submission towards the Partial fulfilment of

BS-MS Dual Degree Program

By

Priyanshu Chandra

Reg. No.: 20131016

Under the guidance of

Prof. Christian Serre

Institut des Materiaux Poreux de Paris

Department of Chemistry

Ecole Normale Superieure Paris (ENS Paris)

Paris – 75005, France

Certificate

This is to certify that this dissertation entitled **"Design and Synthesis of Stable Porous Materials for Sensing Application"** for the fulfilment of BS-MS dual degree program at the Indian Institute of Science Education and Research, Pune carried out by Priyanshu Chandra under the supervision of Prof. Christian Serre at the Institut des Materiaux Poreux de Paris (IMAP) Ecole Normale Superieure (ENS), Paris France and Dr. Sujit K Ghosh at Indian Institute of Science Education and Research (IISER), Pune, India.
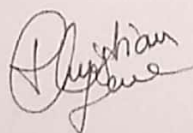
Prof. Christian Serre   **Dr. Sujit K Ghosh**

(supervisor)   (Co-Supervisor)

Professor, Institut des Materiaux   Associate Professor, Department of

Poreux de Paris (IMAP), ENS Paris   Chemistry, IISER Pune

Email: christian.serre@ens.fr   Email: sghosh@iiserpune.ac.in

Signature: Signature:

Priyanshu Chandra

(20131016)

Signature: (Priyanshu Chandra)

Declaration

I hereby declare that the thesis entitled **"Design and Synthesis of Stable Porous Materials for Sensing Application"** submitted for the fulfilment of the BS-MS dual degree program at Indian Institute of Science Education of Research (IISER), Pune has not been submitted by me to any other University or Institution. This work was carried out at the Institut des Materiaux Poreux de Paris (IMAP), Ecole Normale Superieure (ENS), Paris France under the supervision of Prof. Christian Serre and at Indian Institute of Science Education and Research (IISER), Pune, India under the supervision of Dr Sujit K Ghosh.
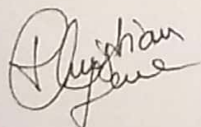
Prof. Christian Serre

(supervisor)

Professor, Institut des Materiaux

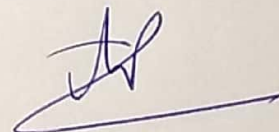Poreux de Paris (IMAP), ENS Paris

Email: christian.serre@ens.fr

Signature:

Dr. Sujit K Ghosh

(Co-Supervisor)

Associate Professor, Department of

Chemistry, IISER Pune

Email: sghosh@iiserpune.ac.in

Signature:

Priyanshu Chandra

(20131016)

Signature: (Priyanshu Chandra)

Acknowledgements

First, I would like to thank my Supervisor, **Prof. Christian Serre** and my mentor **Dr Antoine Tissot** for their advice, guidance and encouragement at all times. I would always be indebted to them for keeping me motivated and helping me develop a scientific outlook. They have been a constant source of inspiration for me.

I must pay my deep regards to my Co-Supervisor **Dr Sujit K Ghosh.** It is SKG lab at IISER Pune where I came to know what MOF means. I joined this wonderful lab when I was in 3rd year of my BSMS. I am thankful to him for keeping faith in me and I am fortunate that I got supervised by him while working on many projects exploring Porous materials. I would like to thank my TAC member **Dr Shabana Khan** for reviewing my project report and her valuable inputs to it.

I would also like to thank all the lab members at IISER Pune and ENS Paris. I learnt a lot from all of them. Especially, **Partha Samanta, Amod V. Desai** and **Dr Florian Moreau**, in gratitude for countless times they have helped me unconditionally.

My friends who provided me constant shipment for fun and joy with a pinch of salt at times. This experience would have had been incomplete without you.

Finaly the people without whom it would not have been possible, My Family (Maa, Papa, Didi & Chhoti). Thank you for being in my life and for being ever supportive.

Dedicated to my beloved Sister

Contents

List of Schemes/Figures

Scheme 1: Synthesis scheme of triazine core.

Scheme 2: Synthesis scheme of PCF-5.

Scheme 3: Dioxin synthesis.

Scheme 4: Nitration of dioxin.

Scheme 5: Reduction of Nitro to the amine.

Scheme 6: H_2-BTDD synthesis.

Scheme 7: Synthesis of Zn-MFU 4l.

Scheme 8: Synthesis of Fe-bpp(COOH).

Scheme 9: Synthesis scheme of Ru-bpp(COOH).

Fig. 1: TGA of PCF-5

Fig. 2: Low temp. N2 adsorption and CO2 adsorption isotherms of PCF-5

Fig. 3: Heat of adsorption curve

Fig. 4: Elemental mapping and EDX of PCF-5.

Fig. 5: Solvent vapour adsorption by PCF-5.

Fig. 6: Images of PCF-5 dipped in different solvents under UV.

Fig. 7: Fluorescent spectroscopy study for PCF-5.

Fig. 8: TGA of PCF-5 after treating with various solvents.

Fig. 9: ^{1}H-NMR for the H_2BTDD ligand.

Fig. 10: ^{1}H-NMR for bpp(COOH).

Fig. 11: PXRD pattern of Fe-bpp(COOH).

Abstract

Chapter 1- One triazine-based ether-linked luminescent porous covalent framework (PCF) has been synthesized. This compound was characterized with infra-red (IR) spectroscopy, thermogravimetric analysis (TGA), field emission scanning electron microscope (FE-SEM) and low-temperature gas adsorption measurements. Further, luminescence-based sensing of the toxic volatile organic compounds (VOCs) has been carried out with the aforementioned compound.

Chapter 2- Two spin crossover complexes {Fe-bpp(COOH), Fe(III)-Sal$_2$tren} and one luminescent Coordination complex {Ru-bpp(COOH)} has been synthesized. These compounds were characterized by Infra-red spectroscopy, Powder-XRD, ^{1}H-NMR spectroscopy. These complexes are encapsulated in a highly stable MOF (Zn-MFU 4l) with a high surface area. Further, these complex-loaded compounds are characterized by Infra-red spectroscopy, Solid-state UV-Visible spectroscopy, FE-SEM, Powder-XRD and Low-temperature gas adsorption studies. Magnetic measurement of the spin crossover complexes and the complex loaded compound has been carried out.

Chapter – 1

A Porous-covalent-Framework for the sensing of Volatile Organic Compounds

1.1 Introduction

It is a very critical and challenging task to distinguish the differences in small structures in molecules for application in environmental monitoring, gas separation and sensor design. A chemo-sensor must be able to detect the differences in various molecules and implement a recognition– transduction protocol.[1-5] Reliable detection of volatile organic compounds (VOCs) is very important for environmental monitoring and health related issues. VOCs are a large group of compounds which are carbon based and they can evaporate or sublimate easily at room temperature. A few typical features of these compounds are: 1) high vapour pressure and low water solubility, 2) boiling point less than 250 °C and 3) Henry's Law constant greater than 0.01 (they should have a tendency to exist in vapour phase).[6] VOCs can be found in the indoor air and their typical sources are paints, wood preservatives, aerosol sprays, air fresheners etc. They can also be found in drinking water sources due to leaking underground storage tanks and also as a result of improper disposal of VOCs containing products. The exposure to VOCs can lead to cancer further it can also cause headaches and central nervous system damage. VOCs detection is also essential in several other applications such as food safety,[7] cosmetic industry[8] and as biomarkers for diagnosis of diseases through breath analysis.[9]

Last decade has witnessed the evolution of porous organic materials in the domain of material science. These compounds have found applications in different fields such as gas storage, gas separation, solvent separation, catalysis, sensing, electrochemical and fuel cell applications etc.[10] Luminescent porous materials have attracted much attention of researchers for their applications as sensors and also in light emitting diodes, biological applications etc.[11] Porous covalent frameworks constitute a subclass of porous organic materials. The high physicochemical stability of such materials has attracted much attention of researchers. Although much research is going on the field of porous organic materials, but sensing of toxic VOCs has been carried out very rarely.

Aromatic VOCs can easily interact with materials having electron rich and deficient moieties via π-π interactions. Thus, we have synthesized one ether linked PCF (PCF-5) having both electron rich and deficient cores inside the network. We then studied the luminescence-based decoding of different organic aromatic VOCs.

1.2 Objective

The objective of this project is to design and synthesize a new functionalized chemically stable porous covalent framework (PCF) for sensing application. Owing to its luminescent properties, volatile-organic compounds (VOCs) sensing can be achieved.

1.3 Methods

1.3.1 Synthesis of 2,4,6-tris(4-fluorophenyl)-1,3,5-triazine

This compound was synthesized by following a previous report.[12] A solution of 4-fluorobenzonitrile (2 g, 16.5 mmol) in dry $CHCl_3$ (10 mL) was added to a solution of trifluoromethanesulfonic acid (triflic acid) (7 mL, 124.6 mmol) in dry $CHCl_3$ (20 mL) at 0 °C under N_2 atmosphere. The reaction mixture was stirred for 2 hours at 0 °C and then at room temperature for 48 hours under N_2 atmosphere. The mixture was then poured into water and unreacted acid has been quenched with saturated solution of sodium bicarbonate. A white precipitate was filtered off and washed with water and chloroform. The product was then dried under vacuum. Yield: 1.7 g, 85%.
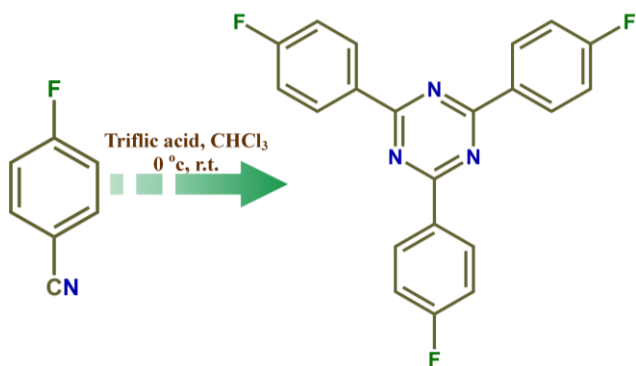
Scheme 1: Synthesis of 2,4,6-tris(4-fluorophenyl)-1,3,5-triazine

## 1.3.2 Synthesis of PCF-5 (Compound-1)

For the synthesis of the PCF-5, 130.6 mg (0.925 mmol) of phloroglucinol and 718.6 mg (5.2 mmol) of K_2CO_3 were dissolved in 20 ml of dimethylacetamide (DMAc) by stirring for 30 minutes under N_2 atmosphere. 500 mg of 2,4,6-tris(4-fluorophenyl)-1,3,5-triazine (1.2 mmol) were dissolved in 20 ml of DMAc and the resulting solution was added dropwise to the reaction mixture and refluxed under N_2 atmosphere for 3 days. Upon completion of the reaction, the precipitate was filtered and washed well with DMAc, Water, dimethylformamide (DMF), tetrahydrofuran (THF), methanol, chloroform, dichloromethane and acetone to remove any unreacted material and small oligomers. Then the collected powder was kept in 1:1 mixture of chloroform and THF for solvent exchange to replace high boiling solvent from the network. PCF-5 was again filtered again and kept at 100 °C under vacuum to remove the guest molecules from the network. Yield: 280 mg
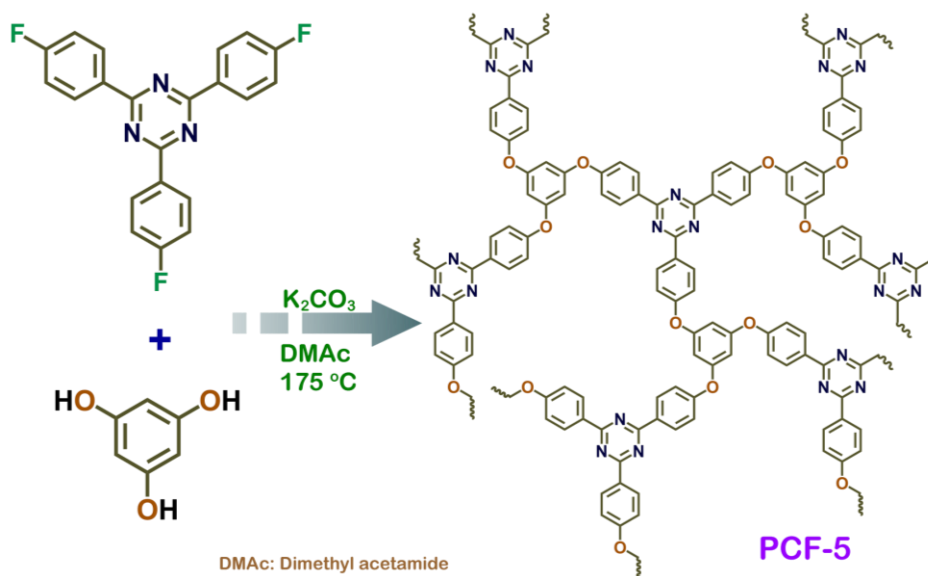
**Scheme 2:** Synthesis of PCF-5 (compound-1)

1.4 Results and Discussions

We have synthesized one triazine-based porous covalent framework (PCF-5) having ether linkage. The compound was characterized by IR-spectroscopy, thermo-gravimetric analysis (TGA) and low-temperature gas adsorption measurements as well as room temperature CO_2 adsorption measurements (at 273 K and 298 K). In addition, Scanning Electron Microscopy (SEM) was employed to investigate the morphology of PCF-5 and EDX analysis was carried out.
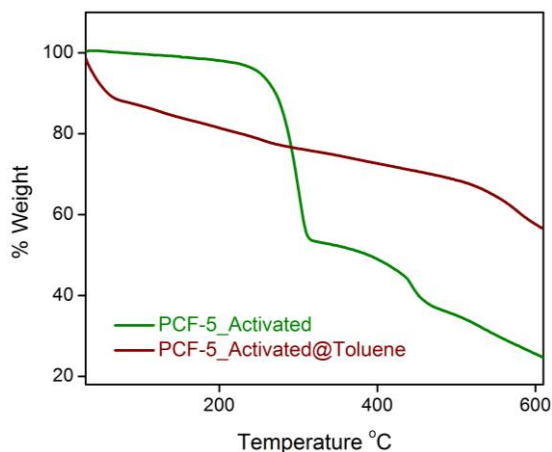

Figure 1: (a) TGA of as-synthesized PCF-5 (wine red) and desolvated PCF-5 (green).

TGA was carried for PCF-5 in order to determine its decomposition temperature. It was found that after activation there is almost no mass loss up to ~ 250 °C then PCF-5 starts to decompose.
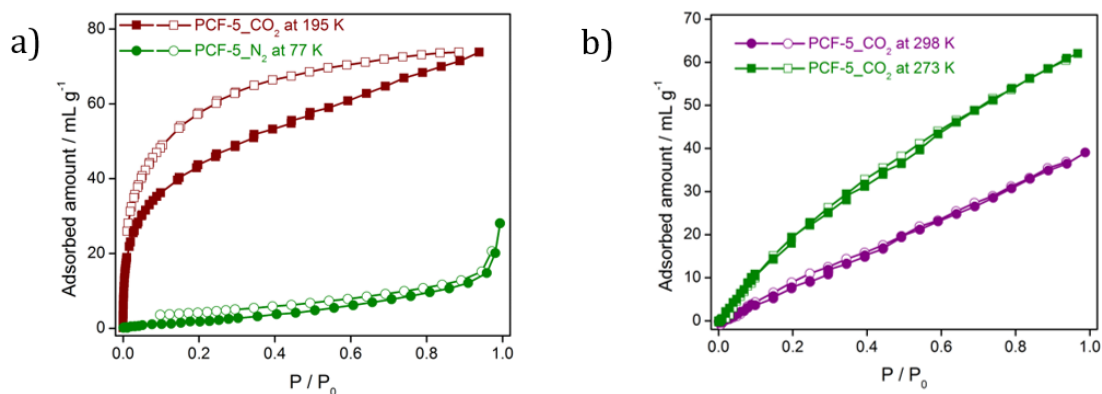
Figure 2: (a) 77 K, N_2 (green) and 195 K, CO_2 (wine red) adsorption isotherms for PCF-5; (b) room temperature CO_2 adsorption isotherms for PCF-5 (green at 273 K and purple 298 K).

Gas adsorption measurements have been carried out at low temperatures for PCF-5. 77K, N_2 adsorption study showed an uptake of ~ 30 mLg^{-1} while CO_2 (at 195 K) uptake was found to be ~ 70 mL g^{-1}. Further, room temperature CO_2 adsorption isotherms were recorded, showing 1 bar uptakes of ~ 62 mL g^{-1} at 273 K and ~ 40 mL g^{-1} at 298 K.
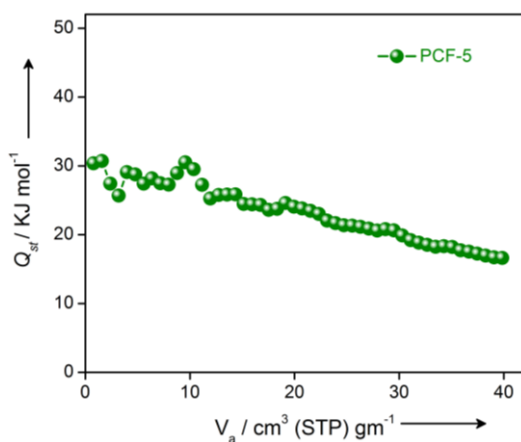
Figure 3: Heat of adsorption (Q_{st}) plot for PCF-5

The heat of adsorption for the PCF-5 is calculated from the data of CO_2 gas adsorption at 273 K and 298 K. It is found to be ~30KJ/mol
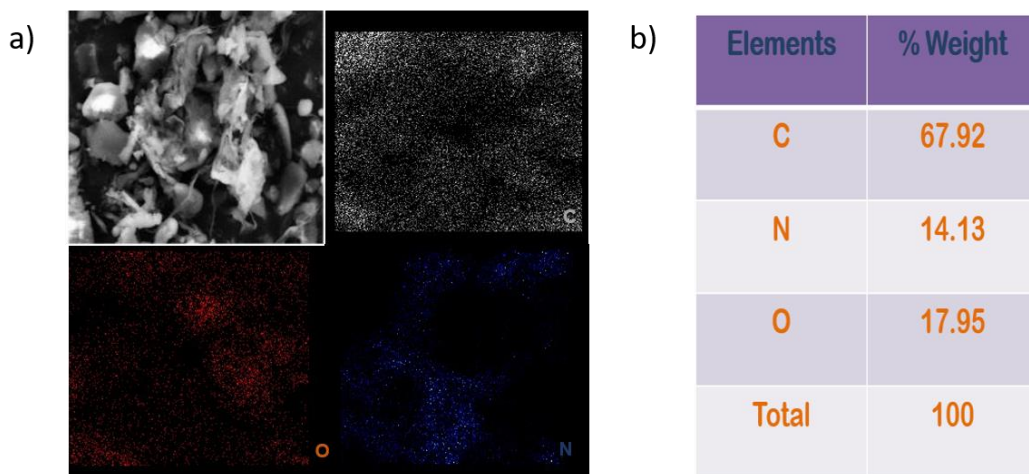
Figure 4: a) Elemental mapping of PCF-5   **b)** EDX analysis of PCF-5.

EDX analysis revealed that the compound was composed of C, N, and O. The elemental mapping of the compound showed that all the elements are homogeneously distributed.
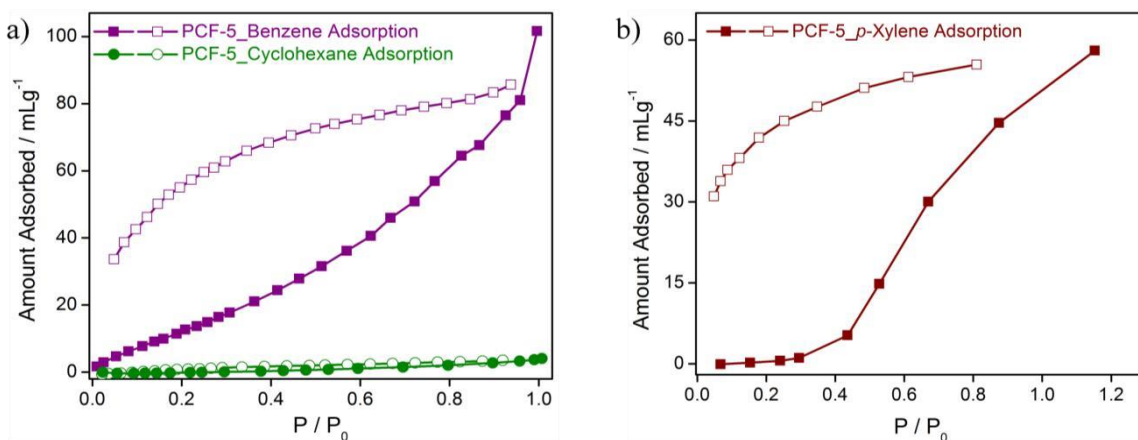
Figure 5: a) Solvent vapour adsorption isotherms for benzene and cyclohexane **b)** Solvent Vapor adsorption isotherm for *p*-xylene.

Solvent vapour adsorption of different VOCs was performed. Interestingly, we could observe a high uptake of Benzene and *p*-xylene compared to that of cyclohexane. Hence PCF-5 may also be used for the separation of these compounds which is a costly process in hydrocarbons industry.
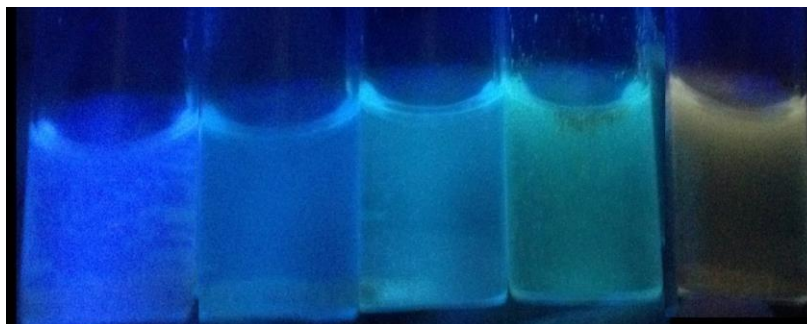
Figure 6: Images of PCF-5 in anisole, p-xylene, benzene, Cl-benzene and cyano-benzene (from left to right) under UV-light.

The compound PCF-5 was loaded with different VOCs and under UV-light, the difference in colour from anisole (blue) to cyano-benzene (orange) could clearly be observed (Fig 7).
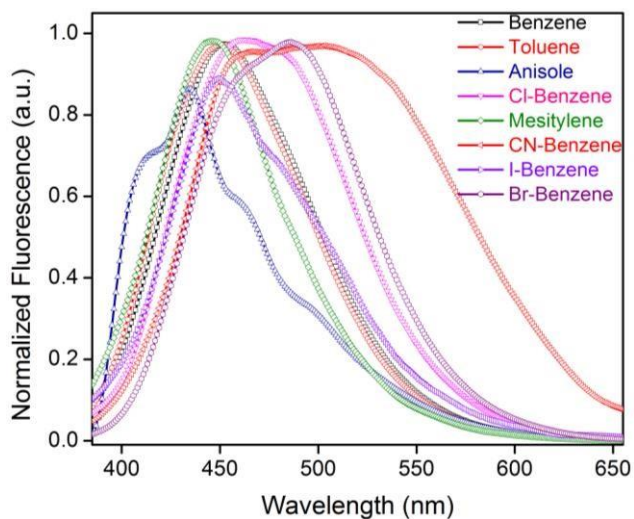
Figure 7: Fluorescence spectra of VOCs loaded PCF-5

We thus performed fluorescence spectroscopy and found a shift in the **λ** max of ~70 nm from Anisole to cyano-benzene. Depending on the electron density of the guest aromatic VOCs the framework interacted differently. Anisole is an electron-rich aromatic compound whereas cyano-benzene is electron deficient.
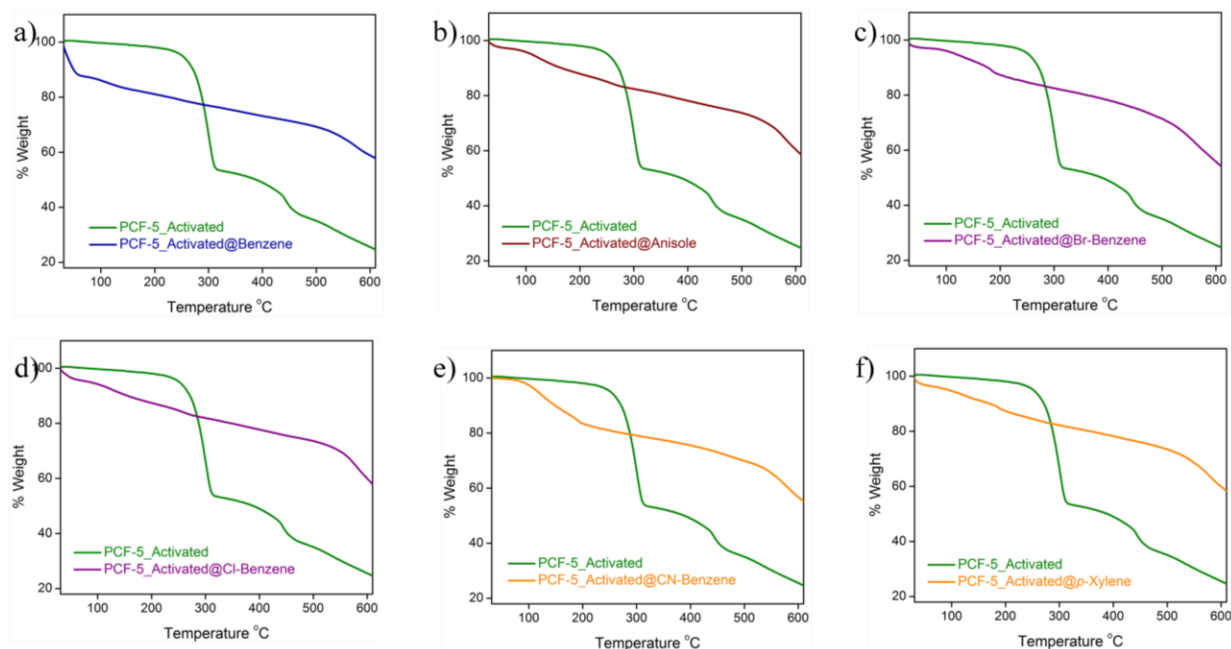
Figure 8: TGA profiles of PCF-5 after treated in different VOCs.

1.5 Conclusion

In conclusion, we have synthesized one luminescent triazine based porous covalent framework (PCF-5) and characterized with IR-spectroscopy, TGA, gas adsorption measurements and SEM. Moreover, fluorescence spectroscopy was performed to explore the sensing ability of the compound towards volatile organic compounds (VOCs). We are now working on confocal imaging of PCF-5 in presence of solvents, quantum yield calculation and thin film preparation of the compound for real-time application.

Chapter – 2

Switchable magnetic/luminescent complex encapsulated Multifunctional materials for sensing application

2.1 Introduction

Spin crossover (SCO) is the phenomenon where the transition of spin takes place from low-spin to high-spin or vice versa due to external stimuli like change in temperature, pressure, magnetic field or irradiation of light. This behaviour is mainly observed in some metal complexes of the first-row transition metal with d^4 to d^7 electronic configuration. SCO was first observed in 1931 by Cambi et al, they discovered anomalous magnetic behaviour for the tris{N, N-dialkyldithiocarbamatoiron(III)} complexes.[13] However, it was the year 1960 when first Co(II) SCO was reported.[14] Now there is interest in looking into the optical and electronic properties of these compounds.[15]

Metal-organic frameworks (MOFs) are a sub-class of porous materials, they consist of metal ion/metal cluster as nodes bridged to each other by organic linkers through coordinate bonds to give rise to a crystalline extended framework with pores of controlled size and shape. MOFs have become an attracting research field in the chemistry community because they exhibit a wide variety of fascinating porous architectures and a large number of physical and chemical properties. These compounds have been widely studied for applications in the fields of gas storage[16], separation[17], catalysis[18], and biomedicine[19], among others. Owing to their porosity, and the possible precise functionalization of their inner surface, MOFs offer a rich host-guest chemistry. Recently, a lot of efforts have been dedicated to the synthesis of functional porous materials, such as luminescent or catalytically active solids. These materials are of special interest in the field of molecular magnetism.[20] To achieve this objective, the encapsulation of coordination complexes in the pores of a MOF is an efficient way to introduce functionality to the material. The synthesis of these solids can be carried out either directly or by post-synthesis insertion of the coordination complex.

2.2 Objective

During this Master thesis project, it is proposed to insert switchable coordination complexes (magnetic or luminescent) in known MOFs in order to obtain porous architectures whose physical properties could be selectively modulated by adsorption of gases or volatile organic compounds. The most interesting solids will then be prepared as thin films to evaluate their potential as sensors.

2.3 Methods

2.3.1 Synthesis of the Ligand (H₂BTDD)

(H$_2$BTDD=bis(1H-1,2,3-triazolo)dibenzo[1,4]dioxin)

The H$_2$BTDD Ligand was synthesized following a previous report.[21]
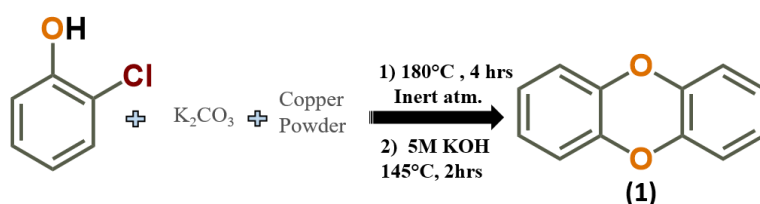
Scheme 3: Synthesis of Dibenzo [1,4] dioxin **(1)**

K$_2$CO$_3$ (55 gram,0.4 mole), and a catalytic amount of copper powder (6 gram) were loaded in a schlenk flask and heated at 100 °C to get rid of the moisture. Then, Chlorophenol (100 gram, 79.1 ml, density 1.264 g/mL) was added to the flask and the resulting tarry mixture was heated at 180 °C under inert atmosphere for 4 hrs. Then the reaction was cooled to room temperature,100 ml of KOH (5 M) solution were added and the mixture was refluxed at 145 °C for 2 hrs. After completion of the reaction, mixture was cooled to room temperature and filtered. The collected solid was washed with DCM (Dichloromethane) and the filtrate was extracted with 500 ml KOH (0.1 M). The organic phase was dried over MgSO$_4$, filtered over a plug of silica gel and then rota-evaporated under vacuum. Then it was recrystallized with ethanol. Yield: 24%
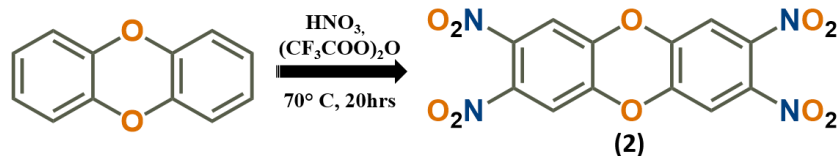
**Scheme 4:** Synthesis of 2,3,7,8-tetranitrodibenzo [1,4]dioxin **(2)**

Fuming nitric acid (24 mL) was added to Trifluoroacetic acid anhydride (16 mL) under cooling in an ice/water bath. **1** (Dibenzo [1,4] dioxin) (5 g, 27.2 mmol) was added slowly, in small portions to a well-stirred nitration mixture while keeping the temperature below 10 °C. The reaction mixture was stirred for 1.5 h at 60-70 °C under reflux and then poured into ice/water (400 mL) with stirring. The precipitate was collected by filtration, washed well with water, and dried under vacuum. Yield:82%
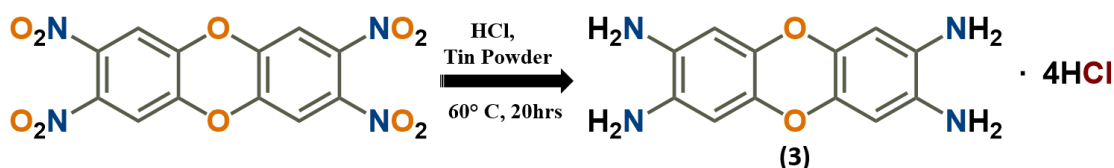
**Scheme 5:** Synthesis of dibenzo [1,4]dioxine-2,3,7,8-tetraamine **(3)**

5 g (10.6 mmol) of nitro compound **2** were charged in a round bottom flask and 215 mL of concentrated HCl was added. Then 62 g (522.4 mmol) of Tin powder was slowly added to the solution, the mixture was stirred at room temperature for 1 hr and then refluxed overnight (60 °C, 20 hrs). Yield:76%
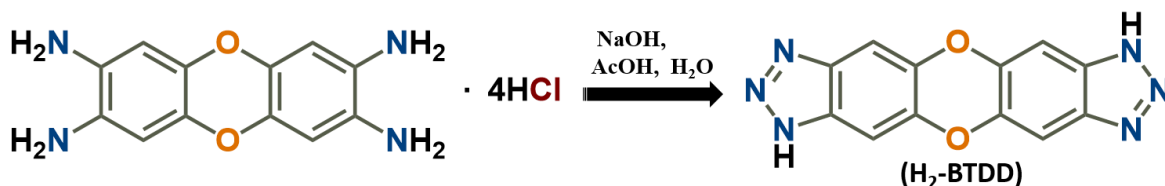
Scheme 6: Synthesis of H$_2$BTDD

The reduced compound **3** (5 g, 14.2 mmol) was added to 50 mL of acetic acid and 7 ml of water. The mixture was well-stirred while kept in an ice bath. Sodium Nitrite (2.03 g, 30 mmol) dissolved in 7 ml water was added to the previously prepared, cooled solution. Then the reaction mixture was diluted with 70 ml water and stirred for half an hour. The precipitate was then removed by filtration, washed well with water and methanol. The obtained powder was then dried under vacuum at 100 °C overnight. Yield:84%
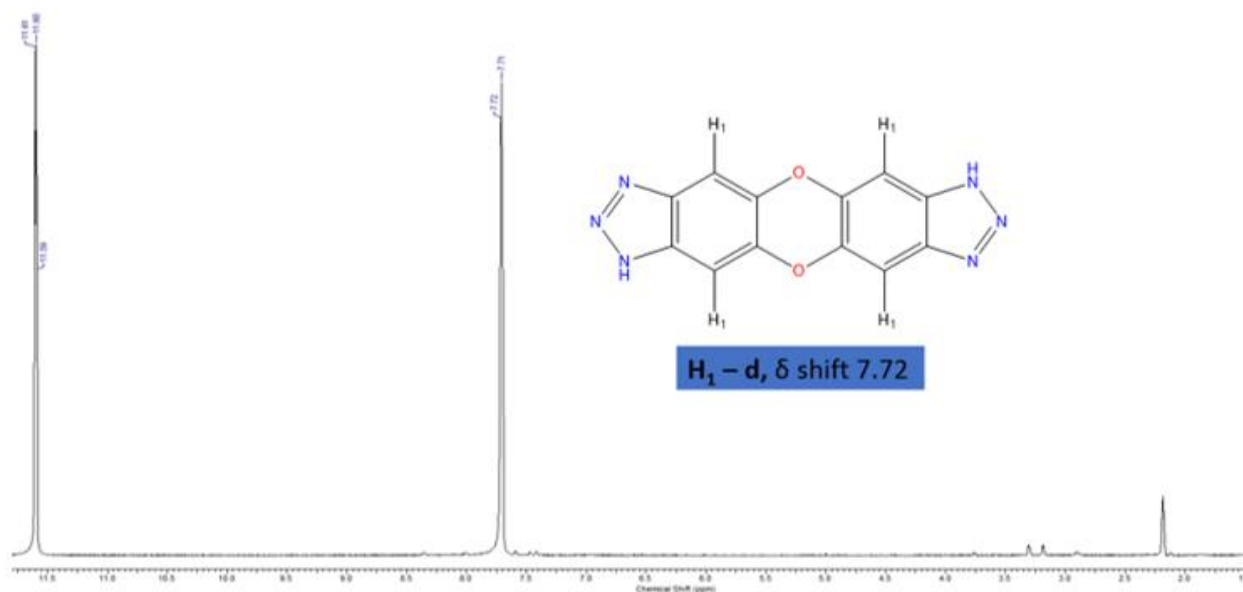
Figure 9: ^{1}H-NMR for the H$_2$-BTDD ligand.

To check the purity of the ligand, ^{1}H-NMR spectroscopy was performed with CF$_3$COOD (Deuterated Trifluoroacetic acid) as a solvent. Since there is just one type of proton present, we see just one peak at a δ shift 7.72 with solvent peak at δ shift 11.5. A small peak at 2.05 is probably due to acetone as the compound was washed with acetone for drying quickly.

2.3.2 Synthesis of Zn-MFU 4I

The Zn MOF was prepared by following a previously reported procedure.[21] H$_2$BTDD (100 mg, 0.364 mmol) was dissolved in 100 ml DMF and heated at 145 °C with stirring. Then the solution was cooled to 50 °C, Zinc chloride (1.02 g, 7.523 mmol) was added to it and it was sonicated till everything is soluble. Then the solution was heated with stirring

under reflux at 145 °C for 18 hrs. The precipitate was then filtered, washed with DMF(3*50 ml), Methanol(3*50 ml), DCM(3*50 ml) and dried under vacuum at 100 °C.

Then we wanted to optimize the reaction condition to improve the crystallinity of the MOF. So, we varied the reaction temperature, metal to ligand ratio, reaction time, added some modulator. Finally, we came up with a scheme which yielded very nice cubical blocked single crystals of the MOF.
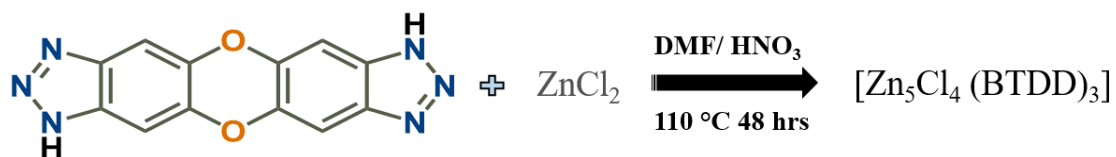
Scheme 7: Synthesis of Zn-MFU 4l.

Revised Protocol- H_2BTDD (10 mg, 0.0364 mmol) was dissolved in 10 ml DMF and heated at 145 °C with stirring. After cooling the solution to 50 °C, Zinc chloride (55 mg, 0.364 mmol) was added, it was sonicated till everything was soluble and one drop of nitric acid was added. The solution was transferred into a small glass vial and kept in oven at 110 °C for two days. After completion of the reaction, the mixture was filtered and the collected powder was kept in hot DMF for 2 hrs (with stirring) to dissolve any unreacted ligand. Then it was solvent exchanged with DCM (Dichloromethane) by using Soxhlet extractor to remove the DMF molecules from the pores of the compound.

2.3.3 Synthesis of the Fe-bpp(COOH) Complex
bpp- [2,6-bis(pyrazole-1-yl) pyridine]

The complex had been synthesized following a similar procedure in a previous report.[22] For the synthesis of bpp(COOH) ; In a 100 mL schlenk flask, Pyrazole (6.13 g, 50 mmol) was put and in a 500 mL schlenk flask Sodium hydride (3.4 g, 142 mol) was put and both the flasks were degassed. Dry DMF was poured into both the flasks to solubilize the solid and Sodium hydride solution was transferred to the other. This was done by connecting both the flasks by a needle and increasing the Nitrogen pressure in the smaller flask. The

flask containing both the solutions was flushed with nitrogen, opened and 2,6-dichloroisonicotinic acid (3g, 15.65 mmol) was added to it and it was closed. Then, it was heated at 130 °C with stirring for 48 hrs. After the competition of the reaction, the mixture was rota-evaporated to remove the DMF. Water was poured into the flask and it was filtered, the precipitate was washed with water till the filtrate became neutral. The collected powder was then dried overnight in the vacuum oven at room temperature. Yield is 84%

In a glass vial, Iron(II) tetrafluoroborate.6 H_2O (33 mg, 0.1 mmol) was solubilized in 2 mL Acetone. In another vial bpp(COOH) powder (57 mg, 0.2 mmol) was solubilized in 10 mL Acetone and the previously made solution was added to it while stirring. The mixture was stirred for 30 min and then kept in a big glass bottle containing Diethyl ether. After one day, red crystals were collected on the wall of the vial.
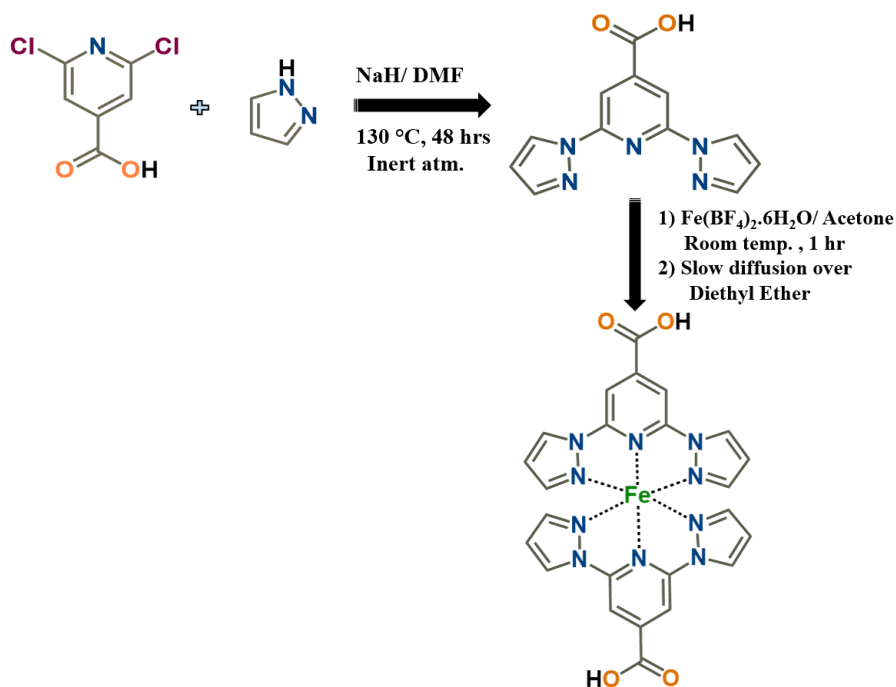
Scheme 8: Synthesis of Fe-bpp(COOH) complex.
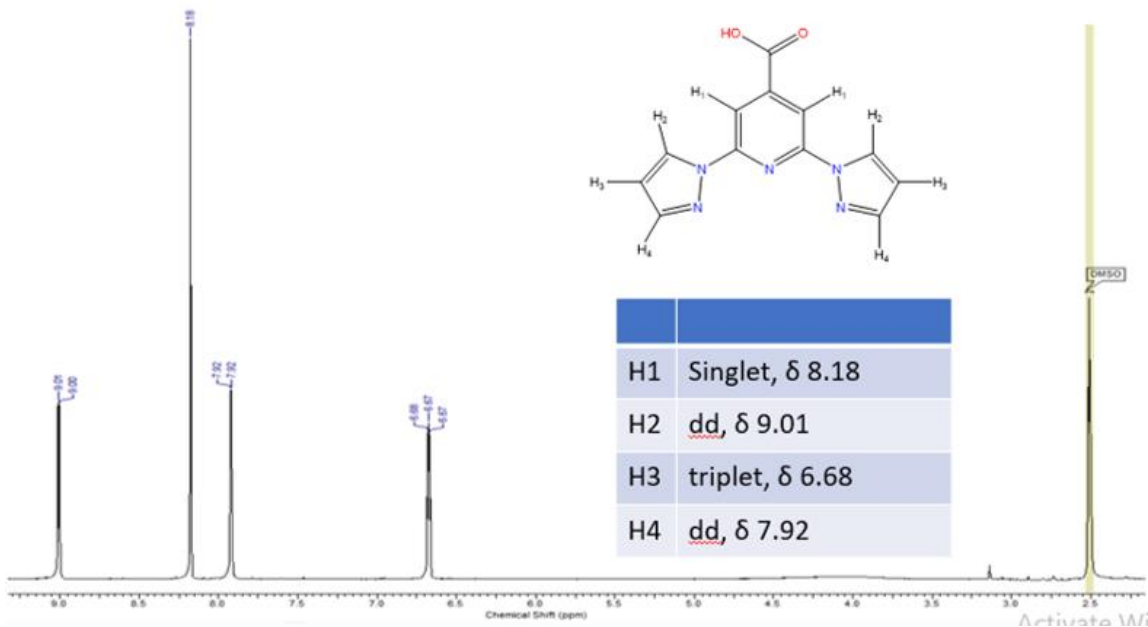
Figure 10: ^{1}H-NMR for the bpp(COOH) ligand.

1H-NMR spectroscopy was performed with DMSO d₆ (Deuterated Dimethyl Sulfoxide) as a solvent to check the purity of the compound. We see four peaks in the spectra as there are four types of protons present in the compound. An extra peak at δ shift 2.5 is due to the solvent.
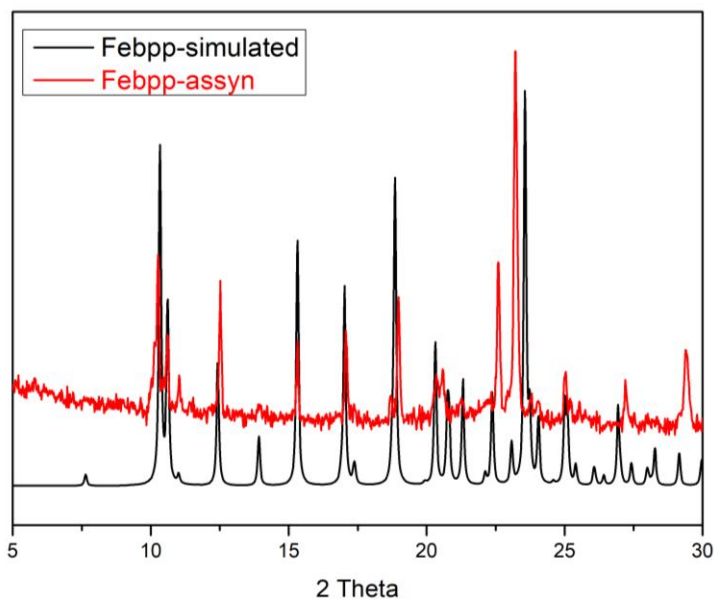
Figure 11: PXRD Pattern of the as-synthesized Fe-bpp complex as compared to the simulated one from SC-XRD.

Unfortunately, the crystals of the Complex obtained after the synthesis were not suitable for SC-XRD. To check the bulk phase purity we compared the PXRD of the as-synthesized complex with the powder pattern simulated from SC-XRD[22] and the pattern matches.

2.3.4 Synthesis of Fe(III) (Sal$_2$tren) Complex

{Sal-Salicylaldehyde, tren- triethylenetetramine}

This Complex was synthesized by a fellow lab member using Salicylaldehyde and triethylenetetramine (trien) following a previous report.[23] I used the as-synthesized compound.
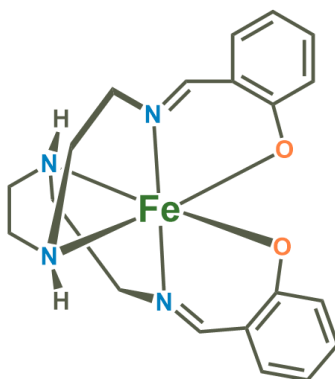
Figure 12: Schematic of Fe(III) (sal)$_2$-tren Complex.

2.3.5 Synthesis of the Ru-bpp(COOH) Complex

A round bottom flask was charged with bpp(COOH) (360 mg, 1.44 mmol) and Ruthenium(III) chloride (150 mg, 0.72 mmol). 30 mL Ethanol was added to the flask and the mixture was refluxed at 70 °C for 48 hrs. Initially, the colour of the solution was black which slowly turned red {probably due to the reduction of Ru(III) to Ru(II)}. After the completion of the reaction, the mixture was cooled to room temperature, filtered and washed with Ethanol. The filtrate was then kept for recrystallization of the complex.
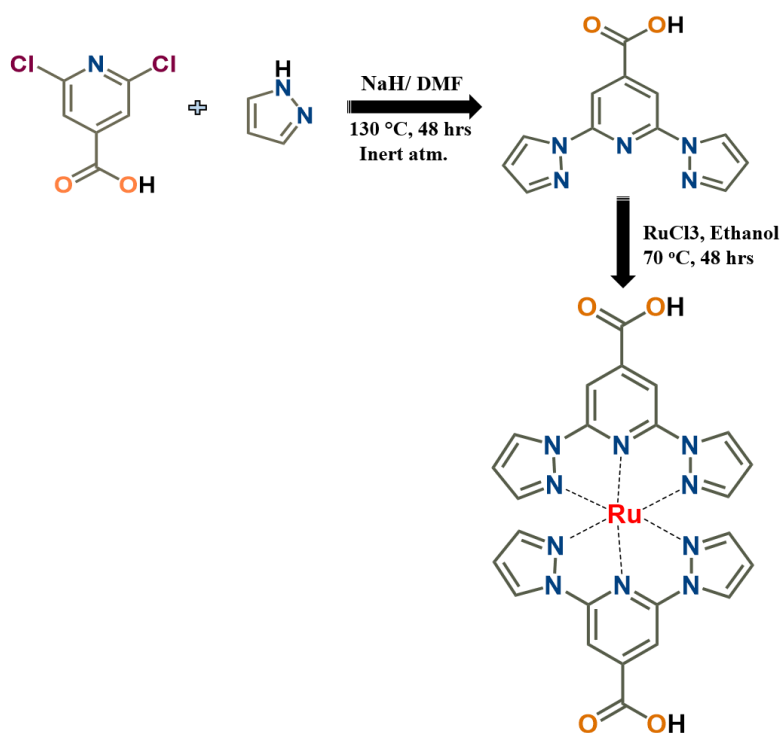
Scheme 9: Synthesis of the Ru-bpp(COOH) Complex.
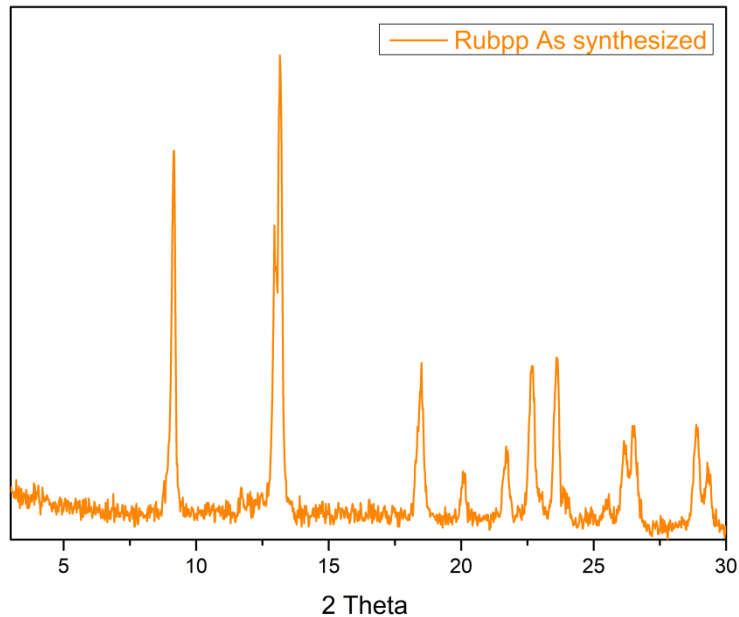
Figure 13: PXRD Pattern of Ru-bpp(COOH) Complex.

The crystals of the complex obtained were not good enough for SC-XRD. We checked the PXRD of the assyn complex and the complex appears to be crystalline with the first peak at 2 Theta = 9.1°

We tried to make MOFs with this Complex and other metals. In the case of Copper(II), We got rod-shaped, green coloured single crystals. But from the SC-XRD measurement, it is found that the Copper ion is replacing the Ruthenium and forming a tetrahedral complex. Copper ion in the complex is coordinated to three Nitrogen from one bpp(COOH) ligand and one chloride ion.

2.4 Results and discussion:-

2.4.1 Characterization of Zn-MFU 4l

For the first characterization of Zn-MFU 4l compound, we performed single crystal XRD measurement. The compound crystallizes in a cubic system. From the structure, we can see that the nodes consist of cationic pentanuclear $[Zn_5Cl_4]^{6+}$ clusters which are connected to each other by $BTDD^{2-}$ linkers. There are two different types of Zinc ions present: One is in tetrahedral coordination geometry surrounded with three Nitrogen from three different BTDD linker (as the base of the tetrahedron) and one chloride (forming the apex of the tetrahedron); Second is in octahedral coordination geometry connected to six Nitrogen from six different BTDD linkers.

Table 1: Structure details of Zn-MFU 4l single crystals.

Chemical Formula	$[C_{36}Cl_4N_{18}H_{12}O_6Zn_5]$
Formula weight	1261.32
Crystal system	Cubic
Space group	Fm-3m(225)
Cell parameter	a=b=c=30.863 Å
Cell volume	29397.8 Å^3
Pore diameter	12.6 Å
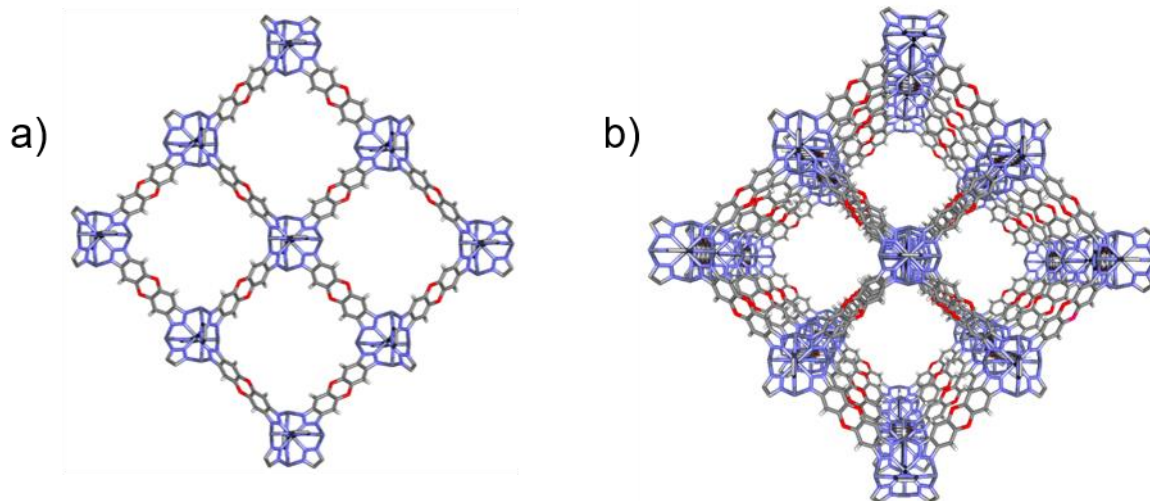
Figure 14: a) Single net structure of Zn-MFU 4l and **b)** perspective view of Zn-MFU 4l.

The chloride ions in the above structures have been omitted just for the clarity of the picture.
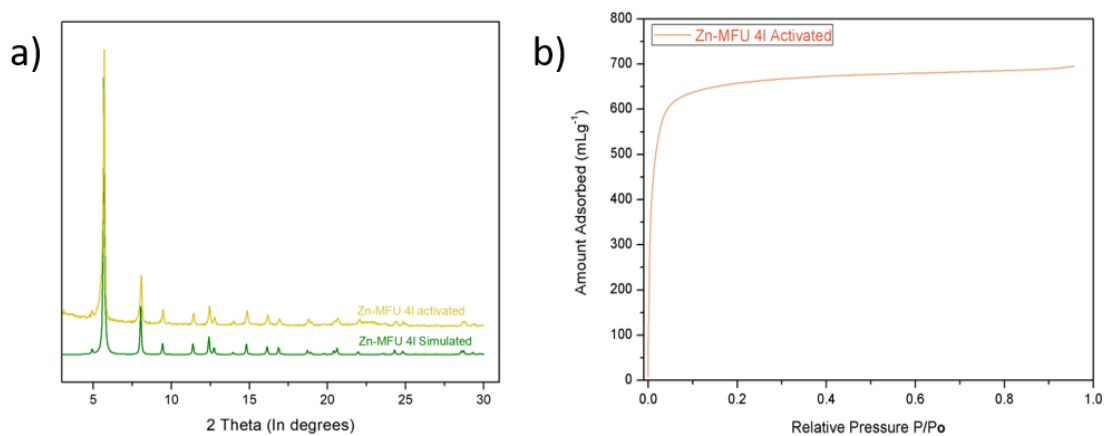
Figure 15: a) PXRD Pattern of as-synthesized Zn-MFU 4l and the one simulated from Single Crystal-XRD **b)** Low temperature (77 K) Nitrogen gas adsorption isotherm for Zn-MFU 4l.

To check the bulk phase purity of the compound, Powder X-Ray Diffraction was performed. The PXRD pattern of the activated compound matches with the simulated one from the Single crystal XRD. The characteristic peaks were at 2 theta values of 5.72° and 8.1° , corresponding to the (2 0 0) and (2 2 0) planes respectively. Further, in order to check the porosity of the compound Low-temperature (77 K) Nitrogen gas adsorption was measured and the compound showed a gas uptake of ~700 cm^3/g. The BET surface area was found to be ~2850 m^2/g which matches with the previous reports.
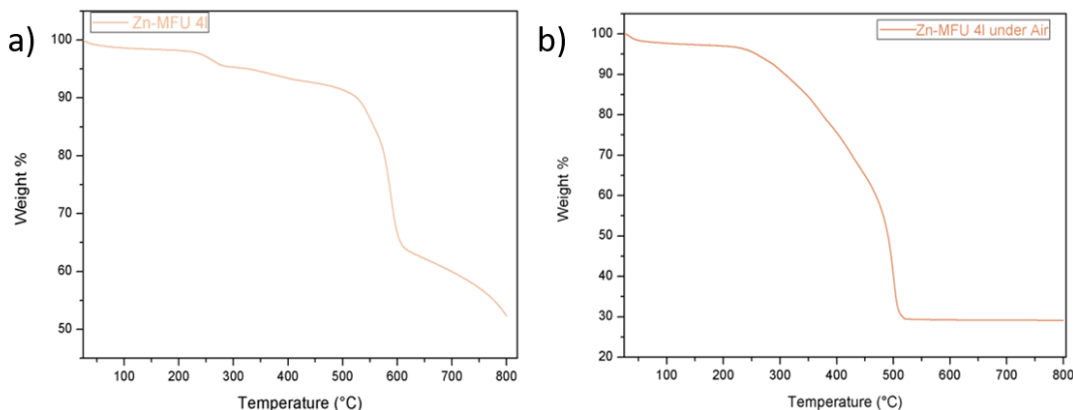
Figure 16: TGA curve for activated Zn-MFU 4I under **a)** N_2 atmosphere and **b)** Oxygen atmosphere.

To check the thermal stability of the compound TGA was performed under nitrogen atmosphere at temperature increasing rate of 10 °C per minute and it is found that the compound is stable up to 550 °C with some loss at 250°C due to decomposition of DMF molecules. However, under oxygen atmosphere, the compound is stable up-to ~300 °C and then it starts to degrade. From here we calculate that there is almost 6.4 % by weight of DMF molecule in the structure.

2.4.2 Encapsulating the Fe-bpp(COOH) Complex in Zn-MFU 4l

In a glass vial, 20 mg of Fe-bpp(COOH) was taken and dissolved in 10 mL acetone. To the solution, 50 mg of Zn-MFU 4l was added and allowed to stir for next 24 hrs. Initially, the colour of the solution was light red but it became less intense after a few hrs of adding the MOF. This demonstrated the encapsulation of the complex visually. After 24 hrs the solution was filtered. The collected powder was washed with acetone several times using centrifuge as the complex is highly soluble in acetone. The filtrate was coloured in first few washes but it became colourless afterwards, ensuring that the complex on the surface of the MOF has been washed. The powder was then dried under vacuum at room temperature. The colour of the powder changed from yellow to brown.
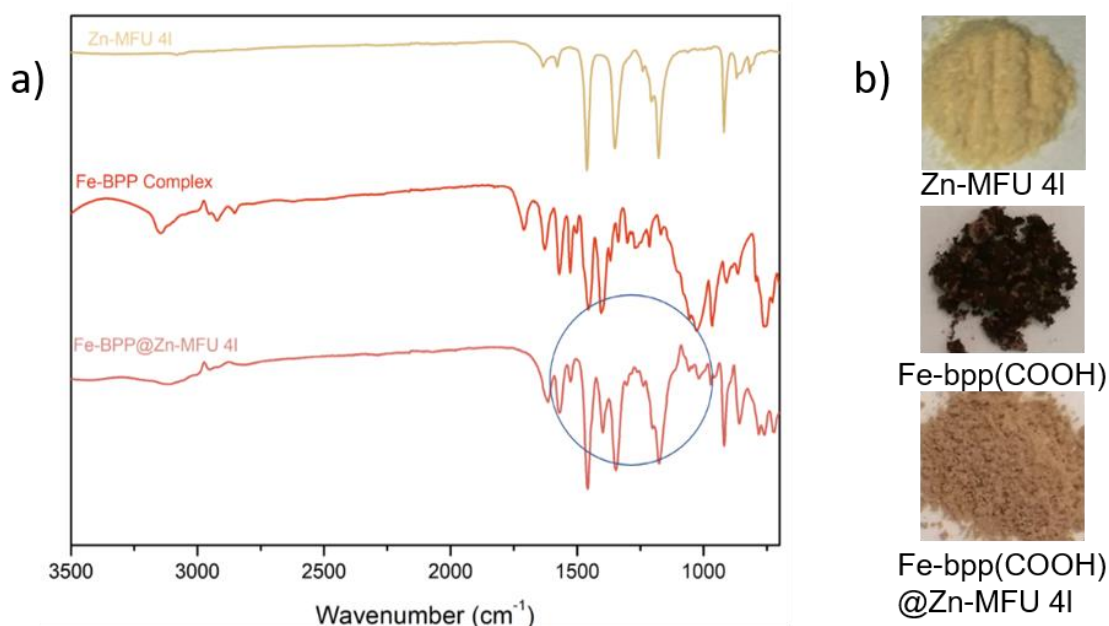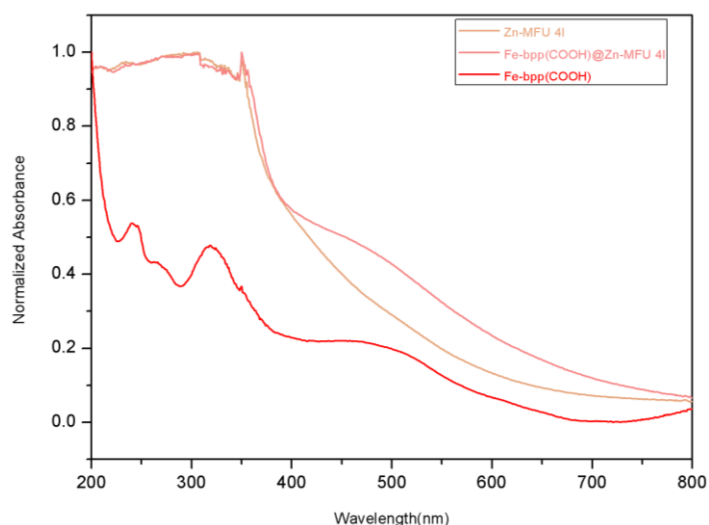

Figure 17: **a)** IR spectra of Zn-MFU 4l (yellow), Fe-bpp(COOH) (Red), Fe-bpp(COOH) @Zn-MFU 4l (Light Red). **b)** images of Zn-MFU 4l, Fe-bpp(COOH) Complex, Fe-bpp(COOH) @Zn-MFU 4l.

To see the loading of the complex in the MOF, we compared the IR spectra of Zn-MFU 4l, Fe-bpp Complex and the Fe-bpp@Zn-MFU 4l. We found that some of the peaks in

the complex observed for the Complex loaded MOF, which evidences the loading of Complex in the MOF.

Figure 18: Solid-state UV-Visible spectra of Zn-MFU 4l (yellow), Fe-bpp(COOH) @Zn-MFU 4l (Light Red).

Solid-state UV-Visible spectroscopy was performed for the MOF and the complex loaded MOF. It showed an absorption peak for the Complex loaded MOF at ~500 nm which is a characteristic Metal to Ligand charge transfer (MLCT) absorption peak for Fe (II) complexes in octahedral geometry (generally red in colour).

Element	Atomic %
Cl	39.39
Fe	7.05
Zn	53.56
Total	100
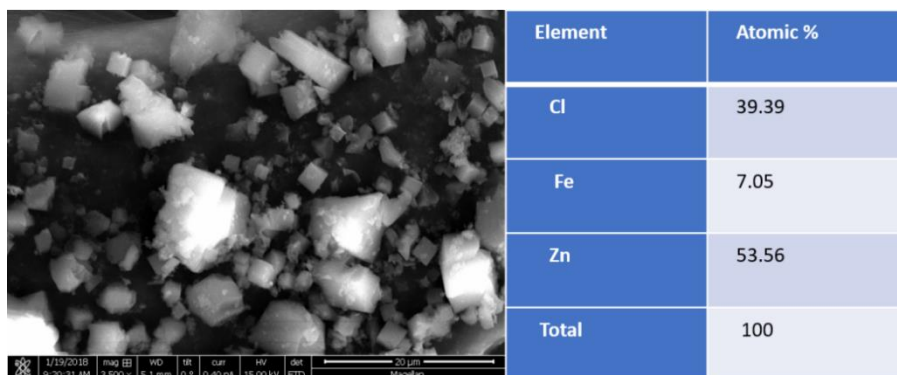
Figure 19: SEM image and EDX analysis of Fe-bpp @Zn-MFU 4l.

FE-SEM and EDX analysis were performed for the complex-loaded MOF. From SEM images, we found that the crystallinity of the MOF is retained after the loading of the complex. From EDX analysis we could calculate that there is ~2.5 complex molecules per unit cell of the MOF.

2.4.3 Encapsulating the Fe-(Sal)$_2$tren Complex in Zn-MFU 4l

In a glass vial 40 mg of Fe-(Sal)$_2$tren was dissolved in 10 mL acetone. 30 mg of Zn-MFU 4l was added to the solution and stirred for 24 hrs. No change in the colour of the solution could be observed because the solution was dark black in colour. After 24 hrs solution was filtered and the powder was collected. The powder was then washed with acetone as the complex is soluble in acetone. This was done to dissolve the complex on the surface of the MOF. After washing, the powder was dried under vacuum at room temperature. The colour of the powder changes from yellow to dark brown.

Figure 20: **a)** IR spectra of Zn-MFU 4l (yellow), Fe(III) Sal$_2$-tren Complex (black), Fe(III) Sal$_2$-tren @Zn-MFU 4l (Dark Brown) **b)** Images of Zn-MFU 4l , Fe(III) Sal$_2$-tren Complex, Fe(III) Sal$_2$-tren @Zn-MFU 4l

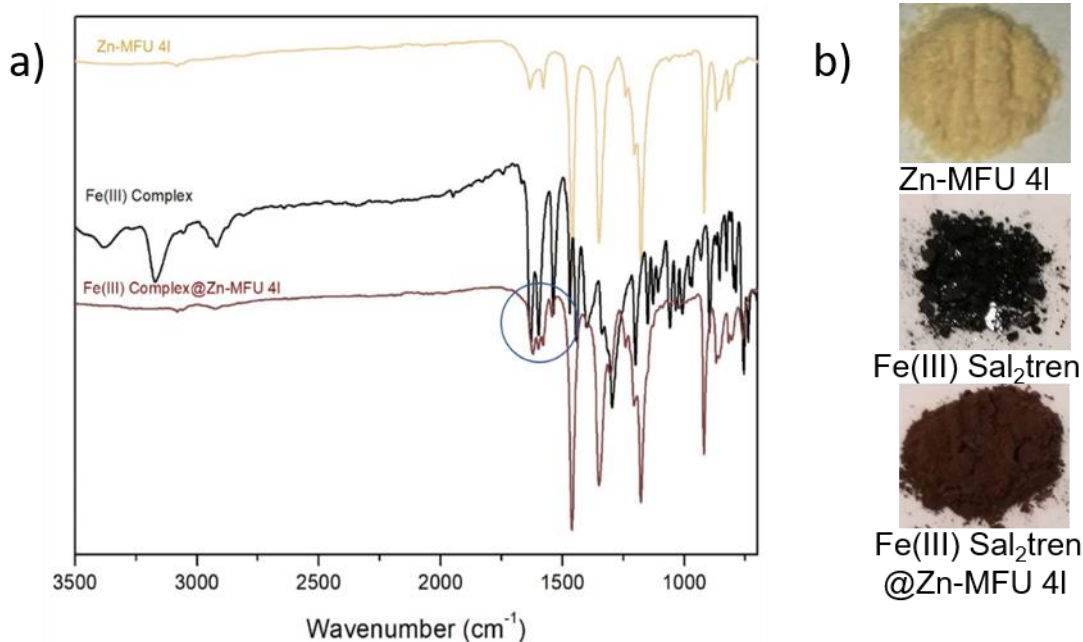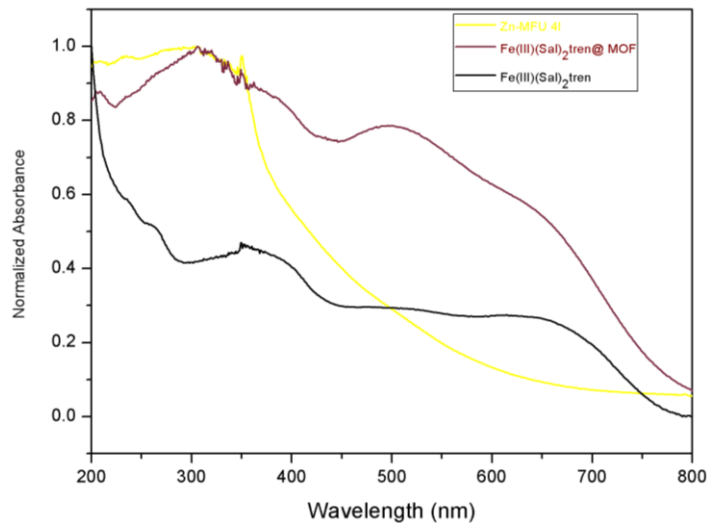IR spectroscopy was performed for the MOF, complex, and the complex loaded MOF. From the spectra, we found that some of the peaks for the complex were also retained for the complex-loaded MOF which illustrated the presence of the complex in it.

Figure 21: UV-Visible spectra of Zn-MFU 4l (yellow), Fe-Sal$_2$-tren @Zn-MFU 4l (Dark brown).

Solid-state UV-Visible spectroscopy was performed for Zn-MFU 4l and Fe-Sal$_2$-tren @Zn-MFU 4l. It has absorption bands at ~520 nm and ~650 nm which are characteristic Ligand to Metal charge transfer (LMCT) peaks for Low-spin and High-spin states of Fe(III)-Sal$_2$-tren complex respectively.

| Element	Atomic %
Cl	24.15
Fe	8.72
Zn	67.13
Total	100
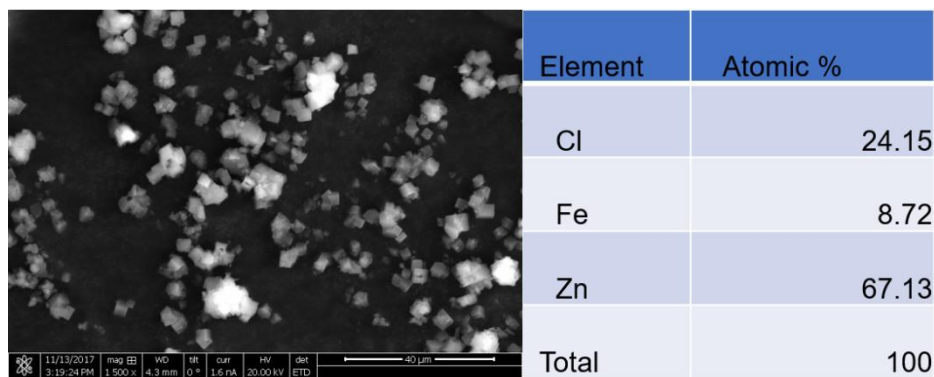
Figure 22: SEM image and EDX analysis of Fe-bpp @Zn-MFU 4l.

From the SEM images, we could see that the loading of the complex was not affecting the crystallinity of the MOF. From EDX analysis we could calculate that there is ~2.6 complex per unit cell of the MOF.

2.4.4 Encapsulating the Ru-bpp(COOH) Complex in Zn-MFU 4l

In a glass vial, 20 mg of Ru-bpp(COOH) complex was taken and dissolved in 20 mL Ethanol. To the prepared solution, 40 mg Zn-MFU 4l was added and the mixture was allowed to stir for next 24 hrs. Initially, the solution was orange in colour which turned colourless after a few hours of adding the MOF. This change in the colour of the solution demonstrated the adsorption of the complex in the MOF. After 24 hrs the solution was filtered. Thus collected powder was washed with ethanol to remove the complex on the surface of the MOF. The powder was further dried under vacuum at room temperature.
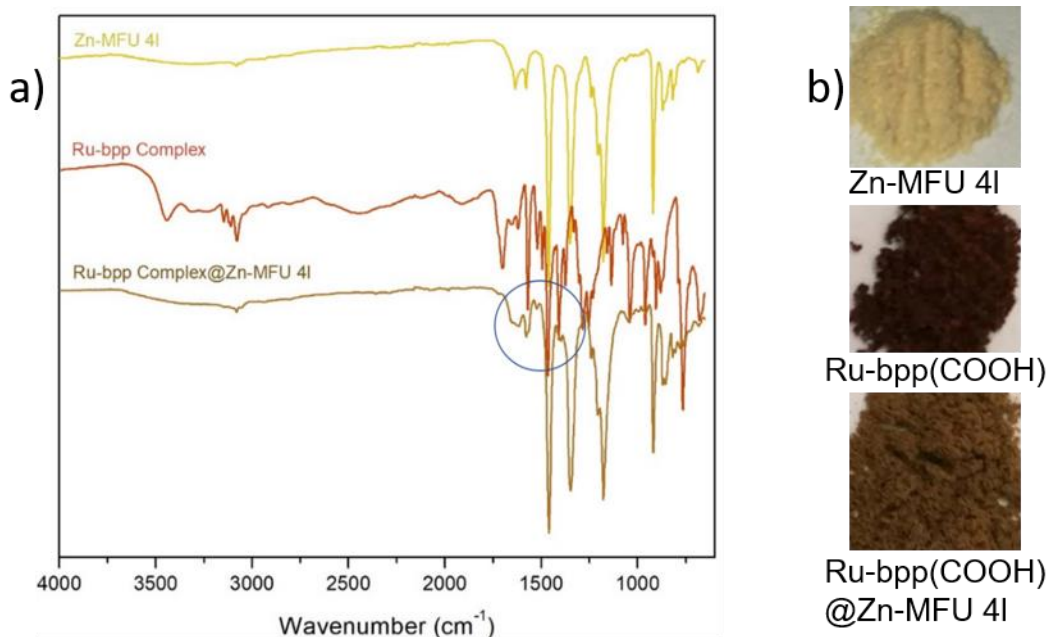
Figure 23: **a)** IR spectra of Zn-MFU 4l (yellow), Ru-bpp(COOH) Complex (wine red), Ru-bpp(COOH) @Zn-MFU 4l (brown). **b)** images of Zn-MFU 4l, Ru-bpp(COOH), Ru-bpp(COOH) @Zn-MFU 4l

Infra-Red spectroscopy was performed for Zn-MFU 4l, Ru-bpp(COOH) Complex and Ru-bpp(COOH) @ Zn-MFU 4l and it is found that some of the peaks from the complex are also retained in the Complex-loaded MOF. It illustrates the presence of the complex inside the MOF.
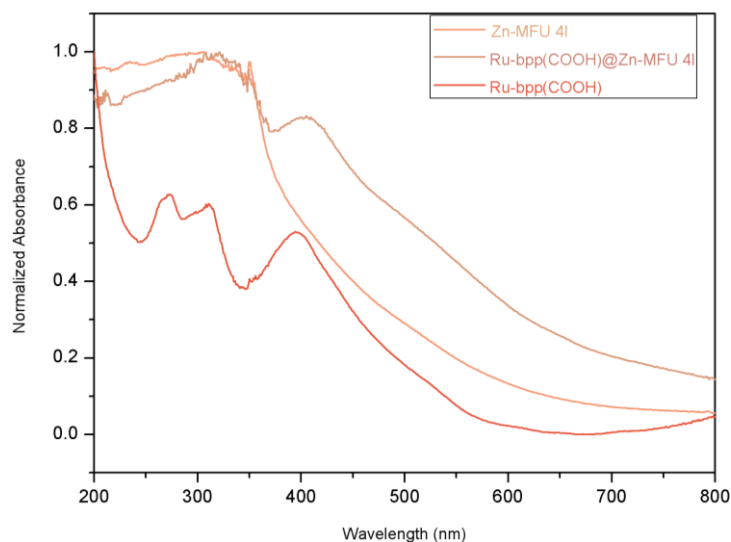
Figure 24: UV-Visible spectra of Zn-MFU 4l (yellow), Ru-bpp(COOH) @Zn-MFU 4l (brown).

In the Solid-state UV- Visible spectra of the Complex-loaded MOF, we can see an absorption band at ~420 nm which is a characteristic of a MLCT band of Ru(II) complexes in octahedral geometry.

Element	Atomic %
Cl	49.62
Zn	47.27
Ru	3.15
Total	100

37

Figure 25: SEM image and EDX analysis of Ru-bpp(COOH) @Zn-MFU 4l.

From the SEM images, we found that the quality of crystal was being a bit affected by the Complex loading, however, the PXRD for this remains unaffected (see next part). From EDX analysis we could see that there is ~1.33 complex loaded per unit cell of the MOF.

## 2.4.5 Further study on the Complex Loaded Zn-MFU 4l
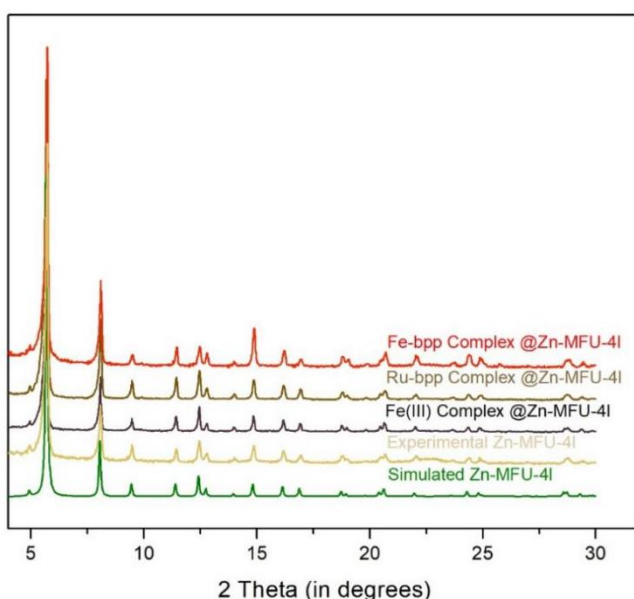
Figure 26: PXRD Patterns of the as-synthesized Zn-MFU 4l loaded with Fe-bpp complex (Red), Ru-bpp complex (Brown), Fe(III) complex (Black), of Zn-MFU 4l as-synthesized (Yellow) and of the simulated Zn-MFU 4l from SC-XRD (Green).

After encapsulating various complexes inside the MOF, we checked the PXRD of all these materials and find that the crystallinity of the compounds remains the same after the encapsulation of these complexes.

Now, we have the Zn-MFU 4l encapsulating different magnetic/luminescent coordination complexes. But these compounds still have to be porous in order to their application for sensing. There should be some space in the pores of the compound so that a guest

molecule can go inside and interact with the complex. For this, we checked the low temperature (77K) N_2 gas adsorption for these compounds.
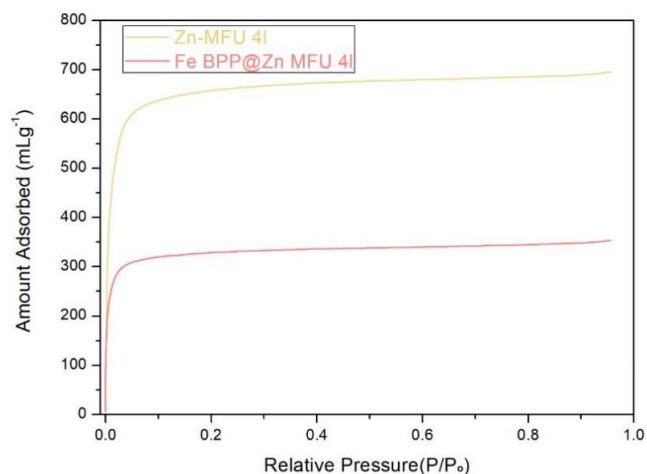
Figure 27: Low temperature (77K) N_2-adsorption isotherms for Zn-MFU 4l (yellow) and Fe-bpp @Zn-MFU 4l (Light Red).

From the low-temperature N_2 gas adsorption isotherm for Fe-bpp @Zn-MFU 4l, we found that the BET surface area of the MOF was reduced from ~2850 m^2/g to ~1350 m^2/g. Which further demonstrated the encapsulation of the complex inside the pore.
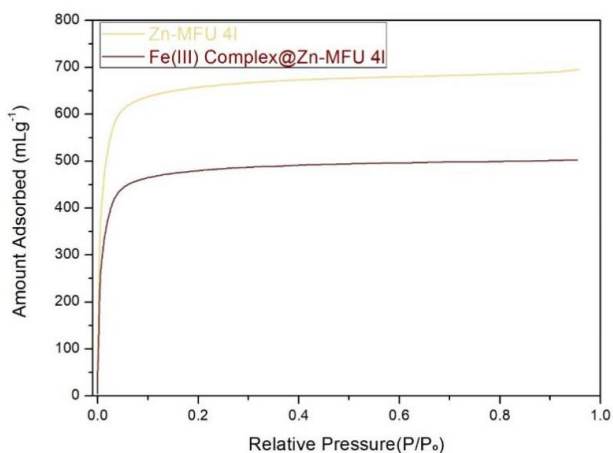
Figure 28: Low temperature (77K) N_2-adsorption isotherms for Zn-MFU 4l (yellow) and Fe(III) sal$_2$tren @Zn-MFU 4l (dark brown)

From the low-temperature N_2 gas adsorption isotherm of Fe(III) sal$_2$tren @Zn-MFU 4l, we found that the BET surface area of the MOF was reduced from ~2850 m^2/g to ~2050 m^2/g. Which illustrated the encapsulation of complex in the MOF.
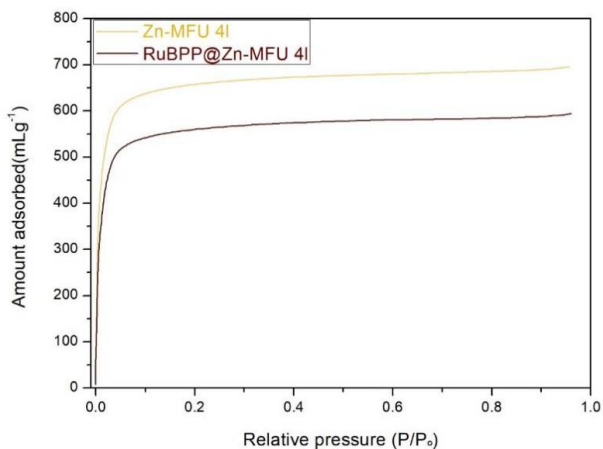

Figure 29: Low temperature (77K) N_2-adsorption isotherms for Zn-MFU 4l (yellow) and Ru-bpp @Zn-MFU 4l (brown).

From the low-temperature N_2 gas adsorption isotherm for Ru-bpp @Zn-MFU 4l, we found that the BET surface area of the MOF was reduced from ~2850 m^2/g to ~2450 m^2/g. It demonstrated the encapsulation of complex inside the porosity.
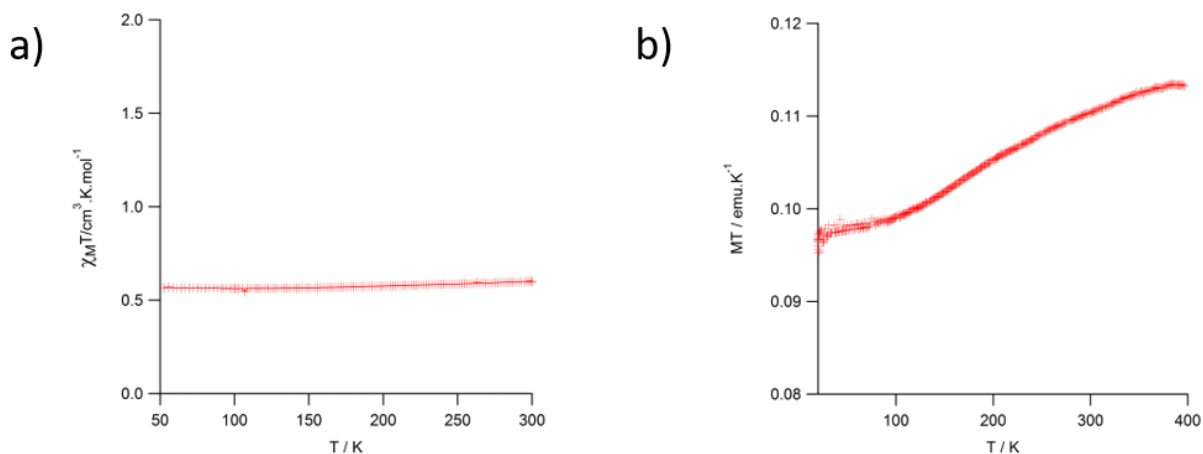
The above adsorption studies strongly suggest the encapsulation of complexes inside the pore of the MOF. At the same time, the complex loaded MOFs still have enough porosity for the inclusion of any guest molecule.

Figure 30: Magnetic measurement of **a)** Fe-(Sal)$_2$tren and **b)** Fe-(Sal)$_2$tren loaded MOF.

From the magnetic measurement studies of Fe-(Sal)$_2$tren we found that it does not show any spin crossover in 50K-300K temperature region which is in accord with the previously reported literature.[24] However, When the complex is encapsulated into the Zn-MFU 4l it shows a increase of the high spin fraction between 150 K and 300 K centered around 220 K, which is probably due to a partial spin-crossover of the complex embedded in the MOF.
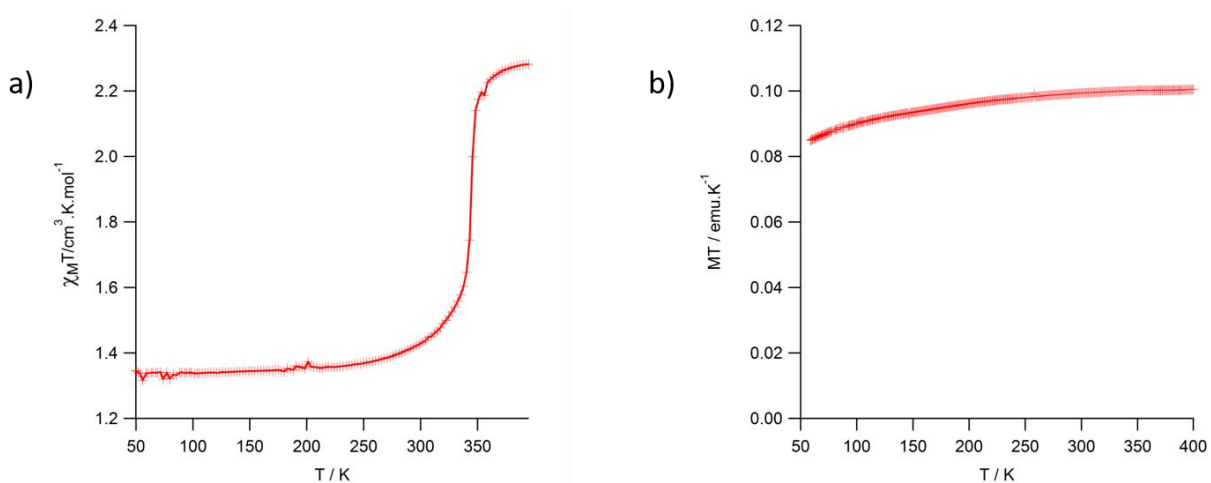
Figure 31: Magnetic measurement of **a)** Fe-bpp(COOH) **b)** Fe-bpp(COOH) loaded MOF.

From the magnetic measurement studies of Fe-bpp(COOH) we found that it shows an abrupt spin-crossover at 344 K temperature region which is again in accord with the previously reported literature.[22] However, When the complex is encapsulated into the Zn-MFU 4l it does not show spin-crossover in the same region of temperature.

Conclusion

In conclusion, we have synthesized two spin crossover complexes {Fe-bpp(COOH), Fe(III)-Sal$_2$tren} and one luminescent Coordination complex {Ru-bpp(COOH)}. These compounds were characterized by Infra-red spectroscopy, Powder-XRD, ^{1}H-NMR spectroscopy. These complexes are then encapsulated in a highly stable MOF (Zn-MFU 4l). Infra-red spectroscopy, Solid-state UV-Visible spectroscopy, FE-SEM, Powder-XRD and Low-temperature gas adsorption studies have been done to characterize the complex loaded compound. Magnetic measurement of the spin crossover complexes and the complex loaded compound has been carried out. Future prospect of this project is to adsorb some VOCs in the pores of the complex loaded MOF and study the change in its magnetic properties.

References:-

1. Haupt, K. et al. Molecularly imprinted polymers and their use in biomimetic sensors. *Chem. Rev*. 100, 2495–2504 **(2000)**.

2. Swager, T. M. et al. Conjugated polymer-based chemical sensors. *Chem. Rev*. 100, 2537–2574 **(2000)**.

3. De Sliva, A. P. et al. Signaling recognition events with fluorescent sensors and switches. *Chem. Rev.* 97, 1515–1566 **(1997)**.

4. Yaghi, O. M. et al. *Nature* 423, 705–714 **(2003)**.

5. Kitagawa, S. et al. Molecular decoding using luminescence from an entangled porous framework. *Nat. Commun.* 2, Article number: 168 **(2011)**.

6. http://www.waterrf.org/resources/Lists/ProjectPapers/Attachments/62/4 457_BackgroundInfo_cVOCs.*Water research foundation* **(2015)**.

7. Khot, L. et al. Development and evaluation of piezoelectric-polymer thin film sensors for low concentration detection of volatile organic compounds related to food safety applications. *Sens. Actuators B*: Chemical 153, 1–10 **(2011)**.

8. Wheals, A. E. et al. Fuel ethanol after 25 years. *Trends in Biotechnology* 17, 482–487 **(1999)**.

9. Peng, G. et al. Diagnosing lung cancer in exhaled breath using gold nanoparticles. *Nat. Nanotechnol.* 4, 669–673 **(2009)**.

10. Wang, W. et al. Covalent organic frameworks (COFs): from design to applications. Chem. Soc. Rev., 42, 548—568 **(2013)**

11. Zhijiang, L. Luminescent microporous organic polymers containing the 1,3,5-tri(4-ethenylphenyl)benzene unit constructed by Heck coupling reaction *Polym. Chem.*,**4,** 1932-1938 **(2013)**

12. Ghosh, S. et al. Enhanced Proton conduction by Post-synthetic covalent modification in a Porous Covalent Framework *J. Mater. Chem. A* 5, 13659-13664 **(2017)**.

13. Cambi, L et.al. Über die magnetische Susceptibilität der komplexen Verbindungen. *Chem. Ber. Dtsch. Ges.* 64, 2591 (**1931**)

14. Hadley B. et al.Unusual magnetic properties of some six-coordinate cobalt(II) complexes' electronic isomers. *J. Am. Chem. Soc.* 83 3732–3734 **(1961)**

15. Dunbar, Kim R. et al. Cyanide-Bridged Complexes of Transition Metals: A Molecular Magnetism Perspective. *Prog. Inorg. Chem.* 56 155–334, **(2009)**

16. Eddaoudi, M. et al. MOF Crystal Chemistry Paving the Way to Gas Storage Needs: Aluminum-Based soc-MOF for CH_4, O_2, and CO_2 Storage *J. Am. Chem. Soc. 137*, 13308–13318 (**2015)**

17. Chen, B. et al. Porous Metal–Organic Frameworks for Gas Storage and Separation: What, How, and Why? *J. Phys. Chem. Lett.*, *5* 3468–3479 (**2014)**

18. Serre, C et al. Synthesis and catalytic properties of MIL-100(Fe), an iron(III) carboxylate with large pores *Chem. Commun.*, 0 2820-2822 **(2007)**

19. *Serre, C.* Metal–Organic Frameworks in Biomedicine *Chem. Rev.*, 112 1232–1268 (**2012)**

20. O. Kahn, Molecular Magnetism, VCH Publishers: New York, (**1993)**

21. Volkmer, D. et al. Elucidating Gating Effects for Hydrogen Sorption in MFU-4-Type Triazolate-Based Metal–Organic Frameworks Featuring Different Pore Sizes *Chem. Eur. J.*, 17, 1837–1848, **(2011)**

22. Coronado, E. et al. A spin-crossover complex based on a 2,6-bis(pyrazol-1-yl)pyridine (1-bpp) ligand functionalized with a carboxylate group *Dalton Trans.*, 43, 9406-9409 **(2014)**

23. Tweedle, M. et al. Fe(III) Chelates with Hexadentate Ligands *J. Am. Chem. Soc.* 4824-4834 **(1976)**

24. Zorina V.L et al. The Highly Conducting Spin-Crossover Compound Combining Fe(III) Cation Complex with TCNQ in a Fractional Reduction State. Magnetochemistry, 3, 9 **(2017)**